GIBBS THEORY OF CAPILLARITY AND POSSIBLE EXISTENCE OF "WETTING PRESSURE"

Sergey Pivovarov
Institute of Experimental Mineralogy, Russian Academy of Sciences
142432 Chernogolovka, Moscow district, Russia
E-mail: serg@iem.ac.ru

ABSTRACT

Paper presents Gibbs theory of capillarity and some estimates for "wetting pressure", i.e., hypothetical repulsive force between solid particles induced by wetting of interfaces.

INTRODUCTION

Capillarity (or capillary action) is elevation or depression of liquids in capillaries, in slits, and in porous media. There are two concepts of interfacial forces: Laplace approach of "surface tension", and Gibbs approach of "surface energy". It is often claimed that these terms are equivalent ("surface tension", N/m = "surface energy", J/m^2). However, this statement leads to numerous contradictions (e.g., see Kaptay, 2011). In spite of this, both approaches coexist in scientific literature even today, with varying prevalence in numerous applications, such as solubility and melting of dispersed substances, nucleation and growth of particles, cloud formation, foam and emulsion stability, etc, etc, etc. Apparent advantage of Laplace approach is consistence with experimental data on capillary elevation. In present study, in order to equate rank of two contradicting approaches, the theory of capillarity was constructed on basis of Gibbs approach. In addition, paper considers relevancy of "wetting pressure", i.e., hypothetical repulsive force between solid particles, induced by wetting of interfaces.

GIBBS THEORY OF CAPILLARITY

The general Gibbs assumption is that the free energy of liquid droplet or solid particle is defined by arithmetic mean free energy of atoms or molecules of dispersed substance. Thus, the excess free energy of the dispersed substance is:

$$G_{ex} = G - G_o = [E_{surf} , J/mol] \qquad (1)$$

Here G is molar chemical potential of liquid droplet or solid particle, G_o is the same for large volume of solid or liquid, E_{surf} is molar surface energy of solid particles or liquid droplets:

$$E_{surf} = \omega \times S \times M = [\omega, J/m^2] \times [S, m^2/g] \times [M, g/mol] \qquad (2)$$

Here $[\omega, J/m^2]$ is specific surface energy of condensed substance (e.g., at 25^oC, it is 0.072 J/m^2 for air-water interface, and 0.465 J/m^2 for air-mercury interface), $[S, m^2/g]$ is specific surface area of liquid droplet or solid particle, and [M, g/mol] is molar weight of dispersed substance.

Eqs. (1, 2) is Gibbs theory of capillarity in compact form, and all capillarity relations may be deduced directly from these equations.

The excess free energy $G_{ex} = G - G_o$ may be expressed as:

$$G_{ex} = G - G_o = RT\Delta ln(\alpha) = RTln(f/f_o) \text{ or } RTln(L/L_o) \tag{3}$$

Here α is "chemical reactivity" of substance, f is fugacity ($\approx$ vapor pressure) above liquid droplets, L is solubility (or solubility product) of solid particles, f_o and L_o are the same properties for the bulk substances, R is gas constant ($= 8.3144$ J/mol°K), and T is absolute temperature (°K). Thus, "chemical reactivity" of substance increases with degree of dispersion as:

$$\Delta ln(\alpha) = \omega \times S \times M/RT \tag{4}$$

Fig. 1 shows data from Stöber (1967) on solubility of quartz at 25°C in 0.155 M NaCl + 0.012 M NaHCO$_3$ (pH = 8.4). Solid curve in **Fig. 1** is:

$$L = L_o \times exp\{0.00552 \times [S, m^2/g]\} \tag{5}$$

Here $L_o = 0.18$ mM is solubility of large quartz crystals. From these data, surface energy of quartz-water interface is $0.00552 \times RT/M = 0.228$ J/m^2. Note here that in accordance with Laplace approach, right side of Eq. (4) should be multiplied by the factor 2/3 (for spherical particles), and Laplace's surface tension of quartz in water is 0.342 N/m. However, there is no data to judge there is the truth.

Radius of solid particle or liquid droplet is related with specific surface area S and density ρ of substance as:
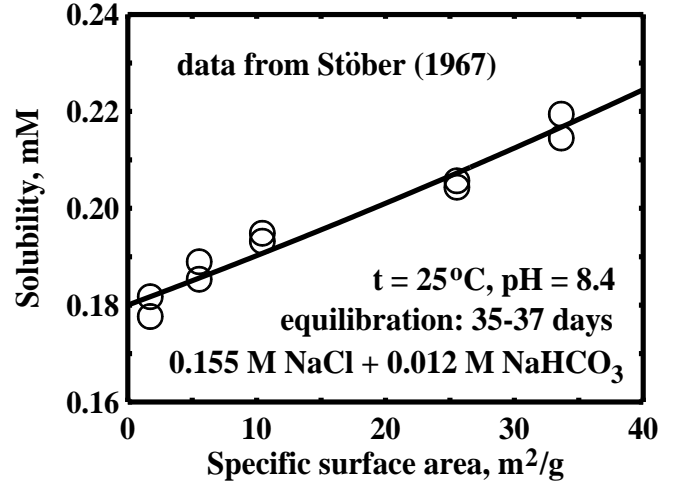

Fig. 1 Solubility of quartz samples with different specific surface area in aqueous solution. Data from Stöber (1967). Solid curve: Eq. (5).

$$r_{sph} = 3/\rho S \tag{6) or}$$

$$r_{sph}, mm = 0.003/\{[\rho, g/cm^3] \times [S, m^2/g]\} \tag{6a}$$

Note that Eq. (6) is valid also for cubic particle (in this case, r_{sph} is a half of side of cube). Thus, for isometric droplets or particles, Eq. (4) may be rewritten as:

$$\Delta ln(\alpha) = (3\omega/r_{sph}) \times \{M/\rho RT\} \tag{7) or}$$

$$\Delta ln(\alpha) = 1.21 \times 10^{-6} \times [\omega, J/m^2] \times \{[M, g/mol]/[\rho, g/cm^3]\}/[r_{sph}, mm] \tag{7a}$$

Note here that the Laplace approach gives factor 2 instead of 3 in Eq. (7).

Radius of cylindrical body is related with specific surface area and density as:

$$r_{cyl} = 2/\rho S \tag{8) or}$$

$$[r_{cyl}, mm] = 0.002/\{[\rho, g/cm^3] \times [S, m^2/g]\} \tag{8a}$$

Note that Eq. (8) is valid for quadrate-based prism (in this case, r_{cyl} is semi-thickness of prism).

So on, "reactivity" of cylindrical body may be calculated from Eqs. (4) and (8):

$$\Delta \ln(\alpha) = (2\omega/r_{cyl}) \times \{M/\rho RT\} \qquad (9) \text{ or}$$

$$\Delta \ln(\alpha) = 0.807 \times 10^{-6} \times [\omega, J/m^2] \times \{[M, g/mol]/[\rho, g/cm^3]\}/[r_{cyl}, mm] \qquad (9a)$$

Semi-thickness of flat body is related with specific surface area as:

$$r_{fl} = 1/\rho S \qquad (10) \text{ or}$$

$$[r_{fl}, mm] = 0.001/\{[\rho, g/cm^3] \times [S, m^2/g]\} \qquad (10a)$$

Thus, "reactivity" of flat body may be calculated from Eqs. (4) and (10):

$$\Delta \ln(\alpha) = (\omega/r_{fl}) \times \{M/\rho RT\} \qquad (11) \text{ or}$$

$$\Delta \ln(\alpha) = 0.403 \times 10^{-6} \times [\omega, J/m^2] \times \{[M, g/mol]/[\rho, g/cm^3]\}/[r_{fl}, mm] \qquad (11a)$$

In general case, in accordance with Gibbs approach, solubility of ellipsoid (or parallelepiped) particles may be calculated from:

$$\Delta \ln(\alpha) = \ln(L/L_o) = \omega \times (1/r_x + 1/r_y + 1/r_z) \times \{V_m/RT\} \qquad (12)$$

Here r_x, r_y and r_z are semi-axes of ellipsoid (or parallelepiped), and $V_m = M/\rho$ is molar volume of substance.

The "reactivity" of liquid above air-liquid interface decreases with altitude in accordance with Boltzmann law:

$$\Delta \ln(\alpha) = \ln(f/f_o) = - Mg\Delta h/RT \qquad (13)$$

Here f is vapor pressure at altitude Δh, M is molar weight of liquid, and g is acceleration of gravity (9.80665 N/kg).

Because the perpetuum mobile is impossible (see **Fig. 2**), capillary elevation in cylindrical tube may be found from Eqs. (9) and (13):

$$\Delta h = - 2\omega_{l/s} /\rho g r_{cyl} \qquad (14)$$

Here $\omega_{l/s}$ is "apparent" surface energy of liquid at interface with solid, which may be defined as a difference between total surface energy of solid-liquid interface and apparent surface energy of solid in contact with liquid:
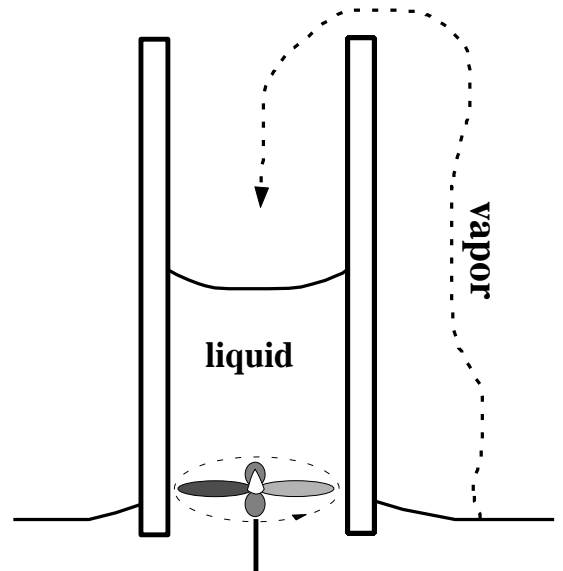
$$\omega_{l/s} = \omega_{tot} - \omega_{s/l} \qquad (15)$$

Fig. 2 Model of perpetuum mobile.

In the absence of interaction between solid and liquid, ω_{tot} is simply a sum of surface energies of air-solid and air-liquid interfaces, $\omega_{tot} = \omega_{liquid} + \omega_{glass}$ (note here that air-substance interface is almost identical to vacuum-substance interface). In such a case, "apparent" surface energy of liquid in contact with solid is equal to surface energy of air-liquid interface: $\omega_{l/s} = \omega_{liquid}$.

Consequently, applying surface energy of mercury $\omega_{Hg} = 0.465$ J/m^2, density of mercury, $\rho_{Hg} = 13.534$ g/cm^3, and g = 9.80665 N/kg, elevation of mercury in glass capillary may be estimated from:

$$\Delta h, \text{ mm Hg} = -\ 7.01/[r_{cyl}\ , \text{mm}] \tag{16}$$

As may be seen, the sign of elevation for mercury is negative, i.e., it is depression. In fact, there is distinctive interaction between mercury and glass, and "apparent" surface energy of mercury in contact with glass decreases.

In **Fig. 3** and **Tab. 1**, the data from Lord Charles Cavendish (as given by Young, 1805) are shown. It should be noted that central depression (which was measured) underestimates the overall effect. In large tubes, central depression (or elevation) fast approaches to zero with radius of tube, whereas marginal depression (or elevation) approaches to constant (see dashed curve in **Fig. 3**). For fine capillaries, this difference is negligible. Solid curve in **Fig. 3** is that calculated by Young (1805) for "mean depression":

$$\Delta h, \text{ mm Hg} = -\ 4.84/[r_{cyl}\ , \text{mm}] \tag{17}$$

Thus, "apparent" surface energy of mercury in contact with glass decreases from 0.465 J/m^2 down to $\omega_{l/s} \approx 0.465 \times (-4.84)/(-7.01) = 0.321$ J/m^2. Because each bond has two ends, similar depression in surface energy (~ 0.144 J/m^2) should be expected for glass in contact with mercury. Consequently, energy of interaction between glass and mercury is ~ 0.288 J/m^2.

Tab. 1 Depression of mercury in glass tubes. Data from Lord Charles Cavendish (as given by Young, 1805). Recalculated, applying 1 Inch = 25.4 mm.

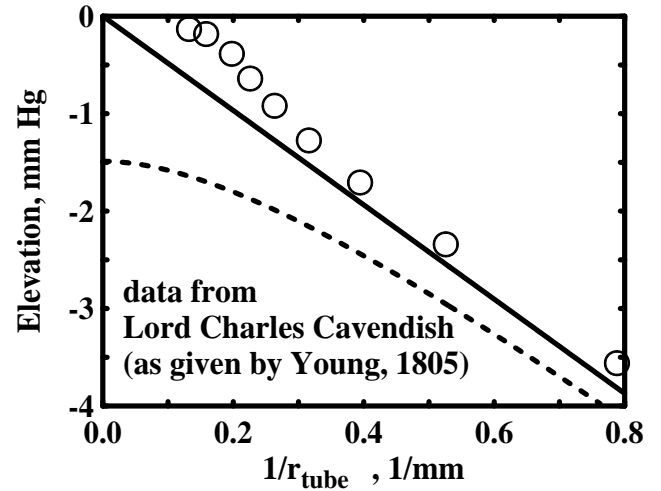| Radius of tube		Elevation	
Inch	mm	Inch	mm
0.3	7.62	−0.005	−0.127
0.25	6.35	−0.007	−0.178
0.2	5.08	−0.015	−0.381
0.175	4.445	−0.025	−0.635
0.15	3.81	−0.036	−0.914
0.125	3.175	−0.05	−1.27
0.1	2.54	−0.067	−1.702
0.075	1.905	−0.092	−2.337
0.05	1.27	−0.14	−3.556

Fig. 3. Central depression of mercury in glass tubes. Data from Lord Charles Cavendish (as given by Young, 1805). Solid and dashed curves: mean and marginal depressions, as calculated by Young (1805).

Similarly, in the absence of interaction between water and walls of tube, elevation of water should be consistent with (see Eq. 14; $\omega_w = 0.072$ J/m^2, $\rho_w = 0.997$ g/cm^3):

$$\Delta h, \text{ mm H}_2\text{O} = -\ 14.73/[r_{cyl}\ , \text{mm}] \tag{18}$$

In fact, the elevation of water in glass tubes is positive (see **Fig. 4** and **Tab 2**):

$$\Delta h, \text{ mm H}_2\text{O} = 13.6/[r_{cyl}\ , \text{mm}] \tag{19}$$

Thus, "apparent" surface energy of water in contact with glass changes its sign, but its absolute value remains approximately the same: $\omega_{w/s} \approx 0.072 \times 13.6/(-14.73) = -0.0665$ J/m^2.

In contact of water with… water, i.e., at complete wetting, apparent surface energy is zero. Thus, change from 0.072 down to -0.0665 J/m^2 is "over-wetting", whereas energy of interaction between glass and water is $\sim 2 \times (0.072+0.0665) = 0.277$ J/m^2. From energy of hydrogen bond (~ 25 kJ per mole of bonds), total number of hydrogen bonds between glass and water is $\sim 0.277/25000 = 11.08 \times 10^{-6}$ mol/m^2 (= number of water molecules in the layer with thickness ~ 2 Å).

Tab. 2 Elevation of water in glass tubes. Data from Weitbrecht (1736). Recalculated, applying 1 Lin = 2.54 mm.

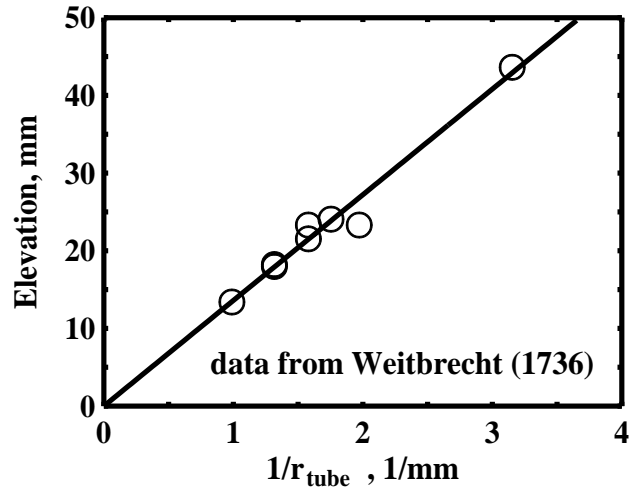| Radius of tube		Elevation	
Lin	mm	Lin	mm
0.4	1.016	5.3	13.46
0.3	0.762	7.1	18.03
0.3	0.762	7.2	18.29
0.25	0.635	8.5	21.59
0.25	0.635	9.2	23.37
0.225	0.5715	9.5	24.13
0.2	0.508	9.2	23.37
0.125	0.3175	17.2	43.69

Fig. 4 Elevation of water in glass tubes. Data from Weitbrecht (1736). Solid curve: Eq. (19)

As may be found from Eqs. (11, 13), elevation of liquid in the slit between two flat surfaces is:

$$\Delta h = -\omega_{w/s}/\rho g r_{slit} \qquad (20)$$

Here r_{slit} is a half of distance between two flat surfaces. Thus, applying the "apparent" surface energy of water in contact with glass, $\omega_{w/s} = -0.0665$ J/m^2 (from data in **Fig. 4**), $\rho_w = 0.997$ g/cm^3, and g = 9.80665 N/kg, one may estimate elevation of water in the slit between two flat glass surfaces:

$$\Delta h, \text{ mm H}_2\text{O} = 6.8/[r_{slit}, \text{ mm}] \qquad (21)$$

As may be seen in **Fig. 5**, Eq. (21) is consistent with observations.

Tab. 3 Elevation of water in slit between two flat glass surfaces. Data from Monge (1787). Recalculated, applying 1 Ligne = 2.2558 mm

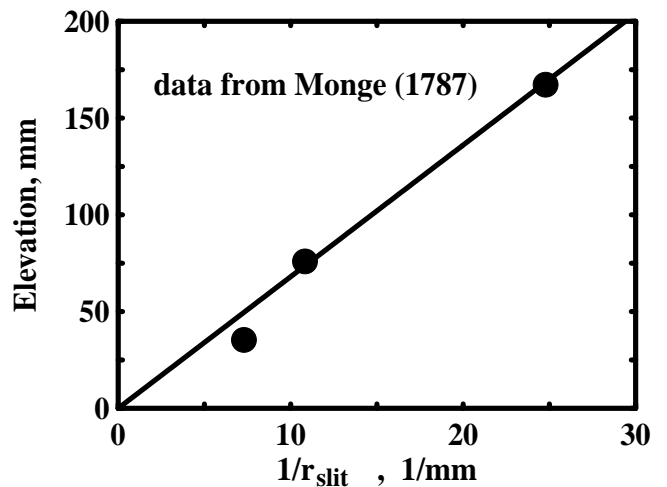| Half of distance between the flat glass surfaces		Elevation	
Ligne	mm	Ligne	mm
2/33	0.1367	15.5	35.0
2/49	0.0921	33.25	75.0
1/56	0.0403	74	166.9

Fig. 5 Elevation of water in slit between two flat glass surfaces. Data from Monge (1787). Solid line: Eq. (21).

Elevation of water in porous medium is somewhat different from that in tubes and slits, because the porous medium acts as a system of capillaries of variable sizes. Above water-saturated zone, water is accumulated in contacts of grains, where the "capillary size" approaches to zero. In result, the intermediate "fringe" zone, where the saturation of pore space with water decreases from 100 % to zero, is extended upward to infinity.

As may be found from Eqs. (4) and (13), capillary elevation of water in porous medium is defined by:

$$\Delta h = - \omega_{w/s} \times S_w / g =$$

$$= - \omega_{w/s} \times S_s \times \{\rho_s / \rho_w g\} \times \{(1-\theta)/\theta\} =$$

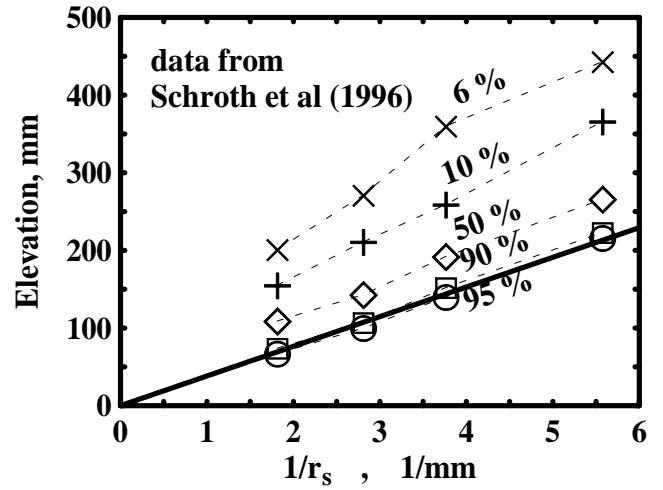$$= - \{3\omega_{w/s}/\rho_w g r_s\} \times \{(1-\theta)/\theta\} \quad (22)$$

Fig. 6 Elevation of water in sand columns as function of grain radius and saturation (interpolated values). Data from Schroth et al (1996). Solid curve: Eq. (23).

Here S_w is specific surface area of water in porous medium, S_s is specific surface area of solid, ρ_s is density of solid particles, θ is porosity, and r_s is radius of solid particles.

Fig. 6 and **Tab. 4** show the data from Schroth et al (1996) on capillary elevation of water in sand columns. Solid curve in **Fig. 6** was calculated from Eq. (22), applying $\omega_{w/s} = -0.0665$ J/m^2 (as for glass-water interface), $\rho_w = 0.997$ g/cm^3, g = 9.80665 N/kg, and $\theta = 0.348$ (the latter value is that measured by Schroth et al., 1996, for all sand columns):

$$\Delta h, \text{mm} = 38.2/[r_s , \text{mm}] \quad (23)$$

As may be seen in **Fig. 6**, Eq. (23) coincides with the head of saturated zone.

Tab. 4 Elevation of water in sand columns (data from Fig. 3 in Schroth et al, 1996; interpolated values). Porosity for all sand columns $\theta = 0.348$.

Radius of grains, mm	Elevation of water, mm, at saturation of pore space:				
	95 %	90 %	50 %	10 %	6 %
0.5525	67	74	109	155	201
0.3565	100	107	143	211	271
0.266	140	152	192	259	360
0.1795	216	223	266	366	443

HYPOTHESIS ON EXISTENCE OF "WETTING PRESSURE"

There is a very old idea on existence of so-called "wetting pressure", or, sometimes, "disjoining pressure" (last term, however, is often used for "electrostatic pressure" between charged interfaces). Many said on pressures arising in opening plant buds, on ability of plant roots to move and crash large stones, etc, etc, etc. Generally speaking, all kinds of such "capillary pressures" may be explained by osmotic or by quasi-osmotic forces. Indeed, sweetness of maple sap was made not for us. Nevertheless, hypothesis on existence of "wetting pressure" may have some relation to reality. Indeed, attraction of water molecules to interface should cause such an effect.

There is so-called "swelling pressure" in clays. In contact with bulk water, clay paste sucks water, and this causes positive pressure, applied to external boundaries of clay body (see **Fig. 7**). Generally speaking, there is no necessity to introduce "wetting pressure" for explanation of this phenomenon. The effect of "swelling pressure" may be explained on basis of simple electrostatic model (see Pivovarov, 2016). Nevertheless, it is possible that the "wetting pressure" gives some contribution into total resistance of clay against compressive force.

Fig. 7 Swelling pressure of clay paste in equilibrium with water.

Fig. 8 shows experimental data on swelling pressure in montmorillonite clay, as measured by Kulchitsky and Usyarov (1981). By analogy with osmotic elevation, one may guess, that the capillary elevation, multiplied by $\rho_w g$, gives hydrostatic pressure, which acts as a force, applied to walls of capillary. Thus, with $S_s = 646$ m^2/g (as measured by Kulchitsky and Usyarov 1981), $\rho_s = 2.78$ g/cm^3 (typical density of clay particles), and $\omega_{w/s} = -0.0665$ J/m^2, one may calculate "wetting pressure" from Eq. (22), multiplied by the factor $\rho_w g$:

$$\Delta P, \text{bar} = 1194 \times \{(1-\theta)/\theta\} \qquad (24)$$

As may be seen in **Fig. 8**, real swelling pressure in montmorillonite clay is 1.5-2 orders smaller than expected from Eq. (24). Thus, "naive model" of "wetting pressure" is totally wrong.
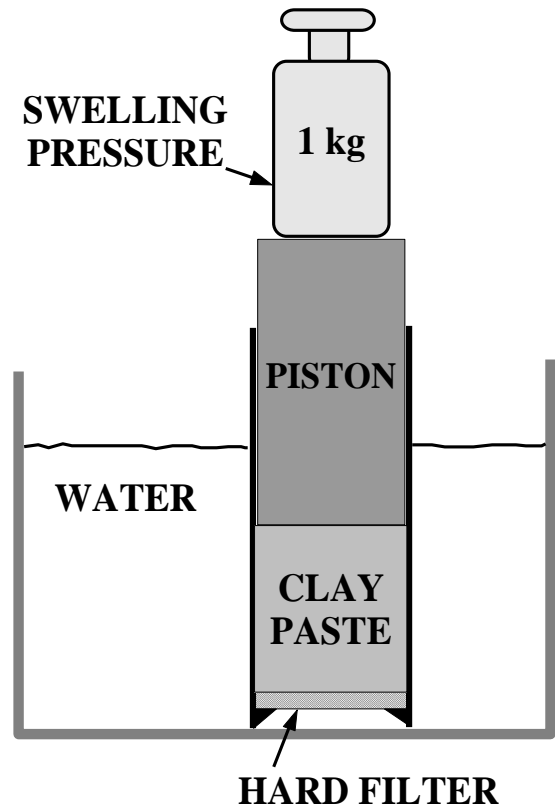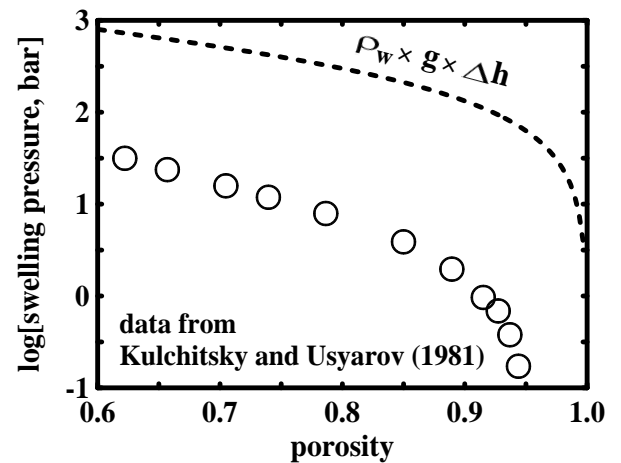

Fig. 8 Swelling pressure in montmorillonite clay (sodium form) equilibrated with water. Data from Kulchitsky and Usyarov (1981). Dashed curve: "naive model" of "wetting pressure" (Eq. 24).

However, it is likely, that the "wetting pressure" exists in very fine capillaries of sub-molecular size. Negative sign of apparent surface energy of water in contact with glass indicates an expansive interfacial force, and thus positive excess pressure at interface. Presumably, attraction between glass and water molecules decreases with distance from interface by exponent. Thus, pressure profile should be consistent with:

$$P_x = P_{x=0} \times \exp(-x/\lambda) \tag{25}$$

Here $P_{x=0}$ is interfacial pressure at $x = 0$ (in the absence of overlap), x is distance from interface, and λ is some specific distance.

Integration of Eq. (25) by dx gives surface energy:

$$\omega_{w/s} = -P_{x=0} \times \lambda \tag{26}$$

It should be noted that $P_{x=0}$ is not "pressure

Fig. 9 Swelling pressure in montmorillonite clay (sodium form) equilibrated with water. Data from Kulchitsky and Usyarov (1981). Dashed curve: "electrostatic pressure" in accordance with Gouy-Chapman model (see for details Pivovarov, 2016). Solid curve: "wetting pressure" (Eq. 29).

jump" between solid and liquid. Attraction of water molecules to solid is equilibrated by attraction of surface atoms to water molecules. In result, "interfacial pressure" acts within a very fine "interfacial layer". However, force fields of interfaces may be overlapped. Thus, "wetting pressure" in flat slit may be estimated as an overlap of interfacial pressures at mid-plane:

$$P_{wet} , \text{bar} = 2 \times P_{x=0} \times \exp(-r_{fl}/\lambda) = -\{2\omega_{w/s}/\lambda\} \times \exp(-r_{fl}/\lambda) \tag{27}$$

Here, r_{fl} is a half of average distance between particles:

$$r_{fl} , \text{Å} = 10000\{\theta/(1-\theta)\}/\{[S_s, m^2/g][\rho_s, g/cm^3]\} \tag{28}$$

In **Fig. 9**, the data on swelling pressure in montmorillonite clay (Kulchitsky and Usyarov, 1981), same as in **Fig. 8**, are plotted on normal scale. Due to significant surface charge (~ - 1.51 $\mu eq/m^2$), electrostatic forces give significant contribution into swelling pressure. Dashed curve in **Fig. 9** was calculated for "electrostatic pressure" in accordance with original Gouy-Chapman model (see Pivovarov, 2016, for details). With specific surface area $S_s = 646 \text{ m}^2/g$, density of particles $\rho_s = 2.78 \text{ g/cm}^3$, and apparent surface energy of water in contact with clay, $\omega_{w/s} \sim -0.0665 \text{ J/m}^2$ (as for glass-water interface), contribution of "wetting pressure" may be estimated from Eq. (27):

$$P_{wet} , \text{bar} = \{13300/[\lambda, Å]\} \times \exp\{-5.57 \times \theta/(1-\theta)/[\lambda, Å]\} \tag{29}$$

The solid curve in **Fig. 9** was calculated from Eq. (29) with $\lambda = 1.5$ Å (which is ~ radius of water molecule). As may be seen, Eq. (29) is not so far from reality as Eq. (24). Thus, it is possible that "wetting pressure" exists in capillaries of sub-molecular size.
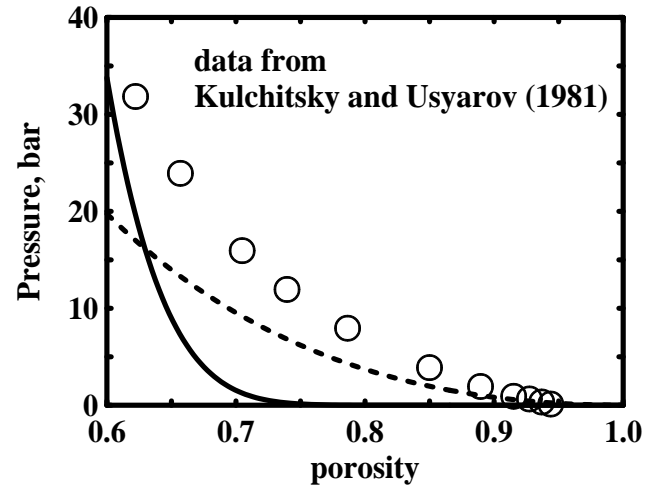
17

CONCLUDING REMARKS

Gibbs approach gives self-consistent theory of capillarity. As for existence of "wetting pressure", this seems to be possible for very fine pores of sub-molecular size. At pore size about of several nanometers, it disappears.

REFERENCES

Kaptay G. (2011) The Gibbs equation versus the Kelvin and the Gibbs-Thomson equations to describe nucleation and equilibrium of nano-materials. J. Nanosci. Nanotech. 12, 1-9.

Kulchitsky L.I. and Usyarov O.G. (1981) Fiziko-himicheskie osnovi formirovaniya svoystv glinistih porod. (Physico-chemical grounds of formation of properties of clay rocks. In Russian.) Moscow, "Nedra".

Monge M. (1787) Mémoire sur quelques effects d'attraction ou de répulsion apparente entre les molécules de matière (Memoir on some effects of the apparent attraction or repulsion between molecules of matter, In French). Histoire de l'Académie Royale des Sciences (History of Royal Academy of Sciences, In French), M.DCCLXXXVII (1787) 506-529.

Pivovarov S. (2016) Swelling pressure in clays. Basis 4, 1-9. (http://basisj.narod.ru/Basis2016_1-9.pdf)

Schroth M.H., Ahearn S.J., Selker J.S., and Istok J.D. (1996) Characterization of miller-similar silica sands for laboratory hydrologic studies. Soil Sci. Soc. Am. J. 60, 1331-1339.

Stöber W. (1967) Formation of silicic acid in aqueous suspensions of different silica modifications. In: Stumm W., ed. Equilibrium concepts in natural water. American chemical society, Washington, D.C., 161-181

Weitbrecht I. (1736) Tentamen theoriae qua ascensus aquae in tubis capillaribus explicatur (Theoretical essay in which the ascent of water in capillary tubes is explained, In Latin). Commentarii Academiae Scientarium Imperialis Petropolitanae (Memoirs of the Imperial Academy of Sciences in St. Petersburg, In Latin) 8, 261-309.

Young T. (1805) An essay on the cohesion of fluids. Philosophical transactions of the Royal Society of London 95, 65-87.